



TECHNICAL REPORT 5

To

The Office of Naval Research
Grant No. N00014-91-J-1414

DTIC
ELECTE
MAR 25 1993
S E D

THE TEMPERATURE DEPENDENCE OF THE
DEFORMATION AND OXIDATION BEHAVIOR OF AN
AGE-HARDENABLE BETA + ALPHA - TWO
TITANIUM ALLOY

D. M. Goto, L. S. Quattrocchi+, and D. A. Koss

Department of Materials Science and Engineering
The Pennsylvania State University
University Park, PA 16802

+Currently: Pratt and Whitney Aircraft
East Hartford, CT 06108

Reproduction in Whole or in Part is Permitted
For Any Purpose of the United State Government
Distribution of this Document is Unlimited



REPORT DOCUMENTATION PAGE		Form Approved OMB No. 0704-0188										
<small>1. Report number, including any institutional or other identification number, should be placed on the front cover of the report. The report number should be placed on the front cover of the report. The report number should be placed on the front cover of the report.</small>												
1. AGENCY USE ONLY (Leave blank)	2. REPORT DATE March 5, 1993	3. REPORT TYPE AND DATES COVERED Technical Report										
4. TITLE AND SUBTITLE The Temperature Dependence of the Deformation and Oxidation Behavior of an Age-hardenable Beta + Alpha-two Titanium Alloy		5. FUNDING NUMBERS										
6. AUTHOR(S) D. M. Goto, L. S. Quattrocchi, and D. A. Koss												
7. PERFORMING ORGANIZATION NAME(S) AND ADDRESS(ES) Dept. of Materials Science and Engineering Penn State University University Park, PA 16802		Report No. 5										
9. SPONSORING MONITORING AGENCY NAME(S) AND ADDRESS(ES) Office of Naval Research 800 N. Quincy Street Arlington, VA		<table border="1" style="width: 100%; border-collapse: collapse;"> <tr> <th colspan="2" style="text-align: left; padding: 2px;">Accession For</th> </tr> <tr> <td style="padding: 2px;">NTIS CRA&I</td> <td style="text-align: center; padding: 2px;"><input checked="" type="checkbox"/></td> </tr> <tr> <td style="padding: 2px;">DTIC TAB</td> <td style="text-align: center; padding: 2px;"><input type="checkbox"/></td> </tr> <tr> <td style="padding: 2px;">Unannounced</td> <td style="text-align: center; padding: 2px;"><input type="checkbox"/></td> </tr> <tr> <td colspan="2" style="padding: 2px;">Justification</td> </tr> </table>	Accession For		NTIS CRA&I	<input checked="" type="checkbox"/>	DTIC TAB	<input type="checkbox"/>	Unannounced	<input type="checkbox"/>	Justification	
Accession For												
NTIS CRA&I	<input checked="" type="checkbox"/>											
DTIC TAB	<input type="checkbox"/>											
Unannounced	<input type="checkbox"/>											
Justification												
11. SUPPLEMENTARY NOTES		<table border="1" style="width: 100%; border-collapse: collapse;"> <tr> <td colspan="2" style="padding: 2px;">By _____</td> </tr> <tr> <td colspan="2" style="padding: 2px;">Distribution / _____</td> </tr> <tr> <td colspan="2" style="padding: 2px;">Availability Codes</td> </tr> <tr> <td style="width: 50%; padding: 2px;">Dist</td> <td style="width: 50%; padding: 2px;">Avail and/or Special</td> </tr> </table>	By _____		Distribution / _____		Availability Codes		Dist	Avail and/or Special		
By _____												
Distribution / _____												
Availability Codes												
Dist	Avail and/or Special											
12a. DISTRIBUTION AVAILABILITY STATEMENT Distribution of this document is unlimited.		<div style="writing-mode: vertical-rl; transform: rotate(180deg);">DTIC QUALITY INSPECTED 1</div> <div style="font-size: 2em; font-weight: bold; margin-top: 10px;">A-1</div>										
13. ABSTRACT <p>The beta Ti alloy Ti-23Nb-11Al (at %) is unique in that it is age hardenable due to the formation of lath-like α_2-phase precipitates based on Ti_3Al. Furthermore age-hardening occurs at temperatures significantly higher than most conventional beta Ti alloys. This suggests the possibility of the elevated temperature usage of α_2-strengthened beta Ti alloys such as Ti-23Nb-11Al. The study examines the compressive deformation behavior of the Ti-23Nb-11Al alloy in the -196°C to 650°C temperature range and demonstrates that very high strengths are possible even at 600°C by precipitation hardening due to the α_2 phase. The thermogravimetric oxidation behavior in laboratory air from 600° to 700°C indicates parabolic behavior consistent with oxygen diffusion through a scale.</p>												
14. SUBJECT TERMS Beta Ti Alloys, Strength, Age Hardening, Oxidation												
17. SECURITY CLASSIFICATION OF REPORT	18. SECURITY CLASSIFICATION OF THIS PAGE	19. SECURITY CLASSIFICATION OF ABSTRACT										

THE TEMPERATURE DEPENDENCE OF THE DEFORMATION AND OXIDATION BEHAVIOR OF AN AGE-HARDENABLE BETA + ALPHA-TWO TITANIUM ALLOY

D. M. Goto, L. S. Quattrocchi* and D. A. Koss
Department of Materials Science and Engineering
The Pennsylvania State University
University Park, PA 16802

Abstract

The beta Ti alloy Ti-23Nb-11Al (at %) is unique in that it is age hardenable due to the formation of lath-like α_2 -phase precipitates based on Ti_3Al . Furthermore age-hardening occurs at temperatures significantly higher than most conventional beta Ti alloys. This suggests the possibility of the elevated temperature usage of α_2 -strengthened beta Ti alloys such as Ti-23Nb-11Al. The study examines the compressive deformation behavior of the Ti-23Nb-11Al alloy in the -196°C to 650°C temperature range and demonstrates that very high strengths are possible even at 600°C by precipitation hardening due to the α_2 phase. The thermogravimetric oxidation behavior in laboratory air from 600° to 700°C indicates parabolic behavior consistent with oxygen diffusion through a scale.

Introduction

Most Ti alloys which retain a predominantly β -phase microstructure after heat treatment are age hardenable due to the formation of hcp alpha-phase precipitates, which occurs in the range of temperatures between 450° and 500°C [1]. However, use of these "conventional" β Ti alloys is limited to temperatures well below precipitation heat-treatment temperatures in order to avoid possible microstructural instabilities. Recent research indicates that it is possible to age-harden the β Ti alloy Ti-23Nb-11 Al (at.%), hereafter designated Ti-23-11, by the formation of lath-like, precipitates based on the ordered intermetallic α_2 -phase Ti_3Al [2,3]. The formation of these precipitate particles in a disordered β -phase matrix results in pronounced age hardening. For example, material in the solution-treated and peak-aged condition exhibits a yield strength about

* Currently at Pratt and Whitney, East Hartford, CT.

600 MPa above that of solution-treated. Furthermore, a significant precipitation hardening increment is retained even after overaging at temperatures as high as 675°C, or about 200°C higher than conventional beta Ti alloys. At these aging temperatures, it is also possible to grow the alpha-two particles to a size wherein fine, uniform slip is induced, probably due to dislocation looping of the particles [3].

The aging behavior of the Ti-23-11 alloy suggests that, after aging in the 575° to 675°C range, the α_2 -phase precipitates will likely be microstructurally stable in the 500° to 600°C range. This should result in the retention of a high level of strength in this temperature regime. However, this is also a range of temperatures where oxidation might limit the performance of a Ti alloy. The purpose of this study is to examine the strength and deformation behavior of the Ti-23-11 alloy over a wide range of temperatures from -196°C to 650°C. The oxidation response in air at 600° - 700°C will also be analyzed on the basis of thermogravimetric data.

Experimental Procedure

The Ti-23-11 alloy had a composition of Ti-22.8Nb-11.1 Al in at. pct. or Ti-38Nb-5Al in wt. pct. The material contained about 1580 wt. ppm oxygen, 160 wt. ppm nitrogen, and 11 wt. ppm hydrogen. Test specimens were machined from bar stock which was extruded at 1038°C using a 22:1 extrusion ratio. All heat treatments were performed by encapsulating Ta-wrapped specimens in quartz under a partial pressure of high purity argon. Prior to specimen machining, the ~25 mm diameter bar stock was solutionized at 1000°C for 1 hour and quenched in ice water. This resulted in a grain size of $\approx 210 \mu\text{m}$, which was unaltered by subsequent aging treatments.

Mechanical tests were performed at elevated temperatures in high purity (99.998%) argon gas in compression on cylindrical specimens 3.17 mm in diameter and length. The compression specimens were electropolished at -40°C in a methanol, ethylene glycol, perchloric mixture [4]. Molydisulfide lubricant was used on the end faces to reduce friction; recent results indicate that this technique effectively produces accurate stress-strain data in compression to strains ≥ 0.5 [5]. The tests were performed at initial engineering strain rates of $3 \times 10^{-4} \text{s}^{-1}$. "Jump" tests, wherein the

strain rate was abruptly increased by $2 \times 10^{-3} \text{s}^{-1}$ and subsequently to $1 \times 10^{-2} \text{s}^{-1}$, were used to determine the strain-rate hardening exponent $m = d \ln \sigma / d \ln \dot{\epsilon}$. Stress changes on both increasing and decreasing strain rates were measured and interpreted as described in detail elsewhere [4].

Isothermal oxidation of the alloy was conducted in flowing laboratory air ($\approx 60 \text{ cc/min}$) between 600° and 700°C . Temperature control was maintained to $\pm 2^\circ \text{C}$. Sample weight was continuously monitored over the oxidation period (≤ 96 hours) by a thermogravimetric analysis device. To facilitate initial surface area measurements, oxidation samples consisted of roughly coupons $\approx 3.75 \text{ mm}$.

Results and Discussion

1. Microstructure

Unlike the microstructures of recent "quasi-beta" alloys such as β -CEZ [6], the microstructure of the Ti-23-11 alloy remains predominantly beta phase even after aging. Hardening during aging at 575° to 675°C occurs by the formation of lath-like precipitates, based on Ti_3Al , in a disordered beta matrix [2,3]. This is accomplished after a solution treatment at 1000°C or about 40°C above the α_2 solvus temperature of $960^\circ \text{C} \pm 15^\circ \text{C}$. The precipitates obey a Burger's orientation relationship with the matrix and retain particle sizes on the submicron scale. For example, aging at 575°C for 6 hours, to peak hardness, results in average dimensions of the lath-like particles of $a \approx 170 \text{ nm}$, $b \approx 120 \text{ nm}$, and $c \approx 30 \text{ nm}$ [2].

Particle coarsening due to elevated temperature exposure is relatively slow in Ti-23-11 alloy. As shown in Figure 1, the maximum dimensions of the particles grow from $\sim 170 \text{ nm}$ after $575^\circ \text{C}/6$ hrs to about 500 nm after 100 hrs at 675°C . The lath-like appearance of the ordered α_2 precipitates suggests coherent or semi-coherent interphase boundaries exist along the broad faces of the precipitate [7]. Since coherent or semi-coherent interfaces generally have low interface migration rates, precipitate coarsening rates are expected to be low. In addition, the coarsening rates of the α_2 precipitates may also be expected to be low due to the somewhat lower rate of diffusion in ordered precipitates. Thus, in comparison to existing β titanium alloys hardened by disordered α -

phase particles, an alloy such as the Ti-23-11 alloy should exhibit superior precipitate stability. This should result in better strength retention to higher temperatures than existing β -titanium alloys.

2. Deformation Behavior

Peak hardness in the Ti-23-11 alloy can be obtained by aging solution-treated material at 575°C for about 6 hrs. However, as shown in Figure 2, a significant degree of age hardening is also possible by aging at temperatures as high as 675°C. In this case, peak hardness is achieved in two hrs, and the hardness increment, 110 VHN, is about half of that (210 VHN) obtained at 575°C.

The temperature dependence of the yield stress for the Ti-23-11 alloy from -196°C to 650°C is shown in Figure 3. It should be recalled that in all cases the alloy was solution-treated at 1000°C prior to aging. Figure 3 indicates that (a) high room temperature yield stresses are possible in this alloy; (b) like other beta Ti alloys [8], there is a strong temperature dependence of the yield stress below room temperature; (c) most of the room temperature yield strength is retained to ~550°C such that the σ_y -T data are nearly athermal; and (d) at temperatures greater than 550°C, a rapid decrease in yield strength with increasing temperature can be observed.

The large degree of age hardening at room temperature in the Ti-23-11 alloy is obtained despite the fact that there has been no alloy development performed to optimize strength. This is the only alloy of this kind that we have tested. The age hardening is obviously a result of the relatively small interparticle spacing achievable during the aging treatments as well as the resistance to the shearing of the ordered Ti_3Al -based particles by mobile dislocations[3].

The strong temperature dependence of the yield and flow stress in bcc alloys at temperatures below room temperature is well known. Owing to a combination of the Peierls stress and interstitial solute effect [8], there is an increase in yield stress $\Delta\sigma_y$ from 27° to -196°C of $\Delta\sigma_y \sim 600$ to 800 MPa. The larger yield stress increase occurs in the solution-treated condition and suggests the presence of thermally activated substitutional solute hardening, probably due to Al atoms. In

other age-hardened β Ti alloy systems, precipitation hardening is found to be athermal and does not affect the temperature sensitivity of the yield stress (i.e., the $\Delta\sigma_y$ value) at low temperatures [9]. Finally, we note that, similar to room temperature observations [3], slip is coarse and planar at -196°C except after aging at 675°C for six hours; in this case the slip was so fine and uniformly distributed that it was unresolvable in an optical microscope.

The yield stress of the age-hardened Ti-23-11 is only weakly sensitive to temperature in the $27^\circ\text{--}500^\circ\text{C}$ range. As before, slip is relatively coarse and planar in this temperature regime except for specimens aged at 675°C . However, as depicted in Fig. 4, the solution-treated material and the specimen aged at 375°C show serrated yielding (or the Portevin-LeChatlier effect) when tested at 327°C . This has been observed previously in β Ti alloys and has been attributed to dynamic strain aging [10,11], probably due to interstitial oxygen.

An analysis of serrated yielding or jerky flow during dynamic strain aging, indicates that the diffusivity (D) of the interstitial atoms is related to strain rate at the onset of serrated yielding such that [12]:

$$D \cong 10^{-9} \dot{\epsilon}. \quad (1)$$

For $\dot{\epsilon} = 2 \times 10^{-4} \text{ s}^{-1}$ and using values for the diffusivity of oxygen in β Ti [13], Eq. (1) predicts the onset of serrated yield to occur at 335°C . This is close to the test temperature of 327°C where the serrations are observed. We also note additional evidence for serrated yield or jerky flow in the negative values of the strain-rate hardening exponent $m = d\log/d\log \dot{\epsilon}$ for the solution-treated alloy ($m = -0.008$) and the alloy aged at 375°C ($m = -0.004$). The specimens aged at 575°C or 675°C did not show serrated yielding; one implication is that the aging treatment reduced the amount of oxygen in solution, decreasing the ability of oxygen to pin dislocations.

As shown in Figure 3, at temperatures greater than $\approx 550^\circ\text{C}$, there is a rapid decrease in yield strength with increasing temperature. Nevertheless, for the specimens aged 2 hrs at 675°C , roughly $\approx 70\%$ of the room temperature yield strength is preserved to 600°C . This is not typical of existing beta-rich alloys which are comparatively much softer (400-600 MPa) in the 600°C

temperature range. Thus, as suggested by the relatively good resistance to particle coarsening described previously, we believe that age hardening as a result of α_2 precipitate formation is a relatively effective means of retaining high strengths in beta Ti alloys to the 500° -600°C range. In the present case, this is achieved by overaging the alloy at 675°C. Aging at 675°C introduces relatively large α_2 precipitates which is known to induce fine, uniform slip as a result of dislocation bypass of the particles. This should be beneficial for ductility of this Ti alloy if intergranular, ductile fracture can be suppressed.

The above observations suggest that the Ti-23-11 alloy has at least short-time precipitate stability at elevated temperatures, up to and including 600°C. However, the stress-strain responses, such as Figure 5 indicate a pronounced tendency for flow softening of specimens aged at 675°C and tested at either 600° or 650°C. Optical microscopy indicates that flow softening is accompanied by the formation of plastic flow localization wherein bands of the microstructure are heavily deformed to create pancake shaped grains with relatively equiaxed bands outside the bands; see Fig. 6.

The cause of the flow softening phenomena in Figure 5 is not well understood. The present strain rates are too slow for adiabatic heating to be the primary cause. Shear banding similar to that observed above has been observed in alpha + beta Ti alloys and was attributed to the possible generation of a softer crystallographic texture, dynamic recrystallization and/or microstructural coarsening [14,15]. In our case, the relative plastic isotropy of the beta phase minimizes any texture softening effects, and no recrystallization was observed. In addition, microhardness measurements within the shear band indicate hardnesses comparable to the adjacent matrix, suggesting no large loss of hardening due to either "damage" to the precipitate particles (or short range order hardening). Thus, although TEM was not performed, we infer from these hardness data that the precipitate microstructure appears to be relatively stable. In support of this, we also note that similar flow softening has been observed in solid solution beta-phase Ti-V alloys at 891°C at high levels of V content (25 and 30%) [16]. Thus this flow softening phenomenon in

Figure 5 appears to be a characteristic of deformation dynamics behavior within the solid solution matrix and not of specific dislocation-precipitate interactions.

The relationship between flow stress and strain rate was examined between 550°C to 650°C and strain rates of $3 \times 10^{-4} \text{s}^{-1}$ to 10^{-2}s^{-1} . Very large ($n > 40$) stress exponents, $n = d \ln \dot{\epsilon} / d \ln \sigma$, were observed in all cases indicating that dislocation glide-controlled processes still dominate deformation. This is not surprising considering that 650° is about 0.5 T_{MP} . It is consistent with the Sherby and Burke [16] observation that power law breakdown creep occurs whenever $\dot{\epsilon}/D_L \geq 10^{13} \text{m}^{-2}$ where D_L is the self diffusion coefficient of the β Ti matrix. In the present case, assuming D_L for self diffusion in β Ti [18], $\dot{\epsilon}/D_L \geq 1.5 \times 10^{13} \text{m}^{-2}$ for all of the test conditions examined. This is consistent with a power law breakdown for the current tests. Testing at temperatures higher than 650°C and at much lower strain rates required to induce steady state creep preferred. The former was precluded by precipitate instability, while the pronounced flow softening discouraged attempts to obtain steady state creep behavior at constant stress through slow strain-rate compressive creep techniques.

3. Tensile Ductility

Owing to a very limited amount of materials, only a few tensile tests were performed. As shown in Table 1, elongation is very sensitive to heat treatment and to the flow stress.

Table I. Room Temperature Ductility Data for the Ti-23-11 Alloy.

<u>Condition</u>	<u>Elongation</u>	<u>Fracture Mode</u>
Solution-Treated (S/T)	22%	Ductile, microvoid fracture; transgranular
S/T + Age 575°C/6hr	~1%	Ductile, slip-band decohesion evident
S/T + Age 675° C/6hr	~3%	Ductile, microvoid fracture; partly intergranular

The minimum ductility (1%) occurred in the peak hardness condition at yield stresses of ~1700 MPa. No effort was made to perform thermo mechanical treatments to optimize ductility.

4. Oxidation Behavior

In addition to creep resistance, the oxidation resistance of titanium alloys is a primary issue regarding their elevated temperature applicability. Beta titanium alloys generally possess poor oxidation resistance, due in part to the presence of the beta-phase stabilizing elements such as vanadium [19]. Recently, replacing vanadium by molybdenum (as the β -phase stabilizer), has improved the oxidation resistance of the β -titanium alloy, Timetal 21s [19]. In the present case, it should be recalled that Ti-23-11 contains a significant amounts of Nb and Al but no V.

Illustrated in Figure 7 is the weight-gain behavior of the Ti-23-11 oxidized in flowing laboratory air over the temperature range of 600° to 700°C for times up to 96 hours. The alloy exhibits parabolic oxidation kinetics, such that weight gain during oxidation may be expressed by the relationship

$$m = \sqrt{k_p t} \quad (2)$$

where m is the weight gain per unit area of original sample, k_p is an effective parabolic rate constant, and t is the time of exposure at the oxidation condition. The continuously increasing sample weight with increasing time implies that a protective oxide scale does not form within the exposure times examined. Furthermore, the Ti-23-11 did not exhibit gross discontinuities in weight gain during oxidation; i.e. no gross transitions in oxidation kinetics were recorded by the thermogravimetric analysis (TGA) equipment. This suggests single stage parabolic oxidation kinetics with no significant changes in the dominant oxidation mechanism over the temperature range and exposure times investigated.

Assuming the oxidation process to be diffusion controlled, the TGA data of Figure 4 can be analyzed in the form of an Arrhenius-type plot. Figure 8 indicates that the effective parabolic rate constant for Ti-23Nb-11Al is

$$k_p = 2.37 \times 10^{13} \exp\left(\frac{-66102}{RT}\right). \quad (3)$$

The activation energy for oxidation ($Q = 66 \text{ kcal/mol}$ or 277 kJ/mol) obtained from Equation 2 corresponds reasonably well with literature values ($Q = 250 - 300 \text{ kJ/mol}$) for oxidation of titanium [20]. Consistent with that behavior, this result tends to indicate that oxidation is rate controlled by oxygen diffusion through a scale.

Inspection of oxidized material (exposed at 600°C for 48 hours) revealed a scale of thickness on the order of $\approx 1 \mu\text{m}$. This is similar to the oxide thickness ($\approx 0.8 \mu\text{m}$) which was observed in the oxidation resistant β -titanium alloy Timetal 21S, (Ti-15Mo-2.7Nb-3Al-0.2Si) which was exposed at 600°C for 72.5 hours in air [21]. The oxidized surfaces of the Ti-23-11 alloy were dark gray to black in color, with occasional patches of a white scale. X-ray diffraction (XRD) identified the white patches as TiO_2 . The dark gray surface scale was not identified, but it is believed to be TiO_2 , based on a similar observation and identification made previously [22].

Finally, Figure 4b also shows a comparison of the parabolic rate constants for the Ti-23-11 alloy with a range of literature values for pure Ti as well as data obtained in our laboratory for the "oxidation-resistant" beta alloy Timetal 21S. The results indicate the Ti-23-11 to be somewhat better than pure Ti. When compared to Timetal 21S, the Ti-23-11 alloy shows similar oxidation behavior in air at 600°C , but it is worse at 700°C .

Summary

This study establishes the concept that, despite the absence of any alloy development, the beta Ti alloy, Ti-23Nb-11Al, can be age-hardened by α_2 -phase precipitates to a high level of strength. Furthermore, the ordered precipitates exhibit comparatively good resistance to particle coarsening phenomena, thus providing at least short-time strength retention to temperatures of $\sim 600^\circ\text{C}$, which is much higher than conventional β Ti alloys. In this temperature range, the Ti-23-11 has similar oxidation resistance in flowing air to the recently developed Timetal 21S.

Acknowledgement

This research was supported by the Office of Naval Research.

References

1. Beta Titanium Alloys in the 1980's, R. R. Boyer and H. W. Rosenberg, eds. (Warrendale, PA: TMS, 1984).

2. L. S. Quattrocchi, D. A. Koss, and G. Scarr Scripta Metall. et Mater., 26 (1992) 267.
3. L. S. Quattrocchi and D. A. Koss, in Proc. to Seventh World Conf. on Titanium, San Diego, 1992.
4. D. Goto, M.S. Thesis, The Pennsylvania State University, 1993.
5. M. Lovato and M. G. Stout, Metall. Trans., 23 (1992) 935.
6. Y. Combres, G. Dumas, A-M. Chaze, and B. Champin in Proc. to Seventh World Conf. on Ti, San Diego, 1992.
7. R. D. Doherty, Met. Sci. 16 (1982).
8. D. A. Koss and J. Chesnutt, R. I. Jaffee and H. M. Burte, eds., Ti Science and Technology (Plenum Press, NY, 1973) p. 1097.
9. S. M. Tuominen and D. A. Koss, Metall. Trans., 6A (1975) 1737.
10. R. Zeyfand and H. Conrad, Acta Metall. 19 (1972) 985.
11. G. Hari Narayanan and T. F. Achhold, Metall. Trans. 2 (1971) 1264.
12. A. H. Cottrell, Dislocations and Plastic Flow in Crystals (Oxford, Clarendon Press, 1953).
13. P. V. Ignatov, L. F. Sokyriansky, M. S. Model and A. Yashinyaev, in Titanium Science and Technology, ed. R. Jaffee, H. M. Burte, (New York: Plenum Press, 1973), p. 2535.
14. P. Dadros and J. F. Thomas, Metall. Trans., 12A (1981) 1867.
15. S. L. Semiatin and G. D. Lahoti, Metall. Trans., 12A (1981) 1705.
16. H. Oikawa in Creep and Fracture of Engineering Materials and Structures, ed. by B. Wilshire and R. W. Evans (London, Inst. of Metals, 1991), p. 31.
17. O. D. Sherby and P. M. Burke, Prog. Mater. Sci., 13 (1967) 325.
18. H. Oikawa, K. Nishimura and M. X. Cui, Scripta Metall., 19 (1985) 825.
19. P. J. Bania, ISIJ Int., 31 (1991) 840.
20. Z. Liu and G. Welsch, Metall. Trans. A, 19A (1990) 1121.
21. T. A. Wallace, R. K. Clark and K. E. Wiedemann in Seventh World Conf. on Titanium.
22. J. Stringer, Acta Metall., 8 (1960) 758.

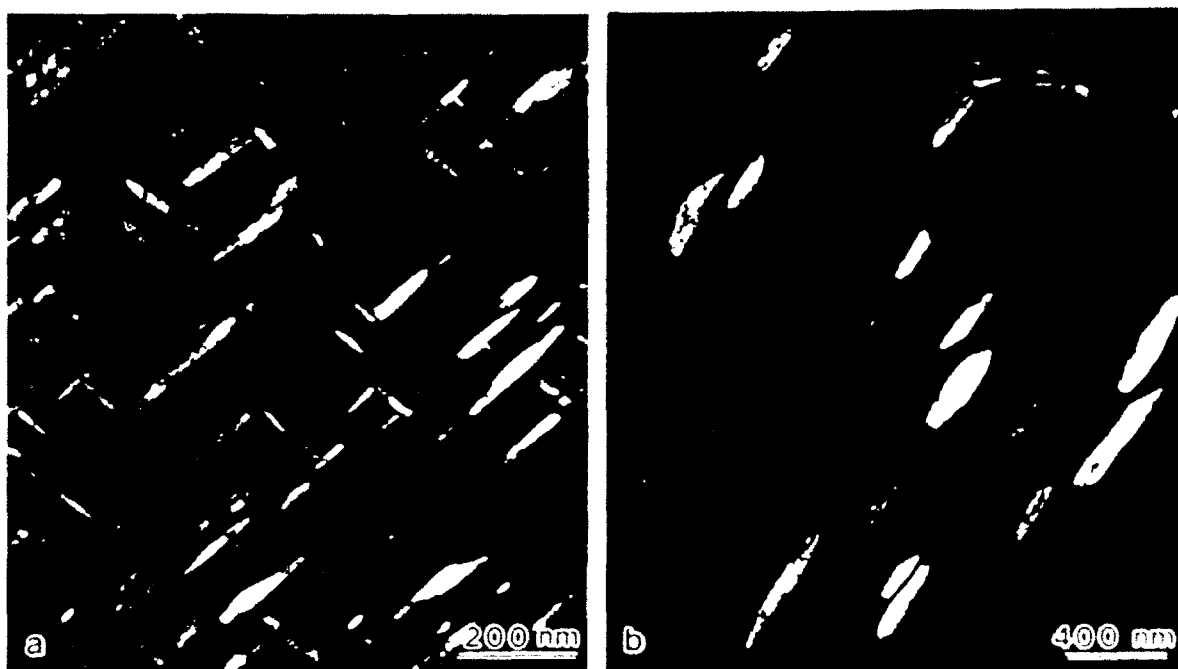


Figure 1. CDF image of the α_2 -phase precipitates formed when the Ti-23-11 alloy was aged (a) at 575°C for 6 hours and (b) at 675°C for 100 hrs.

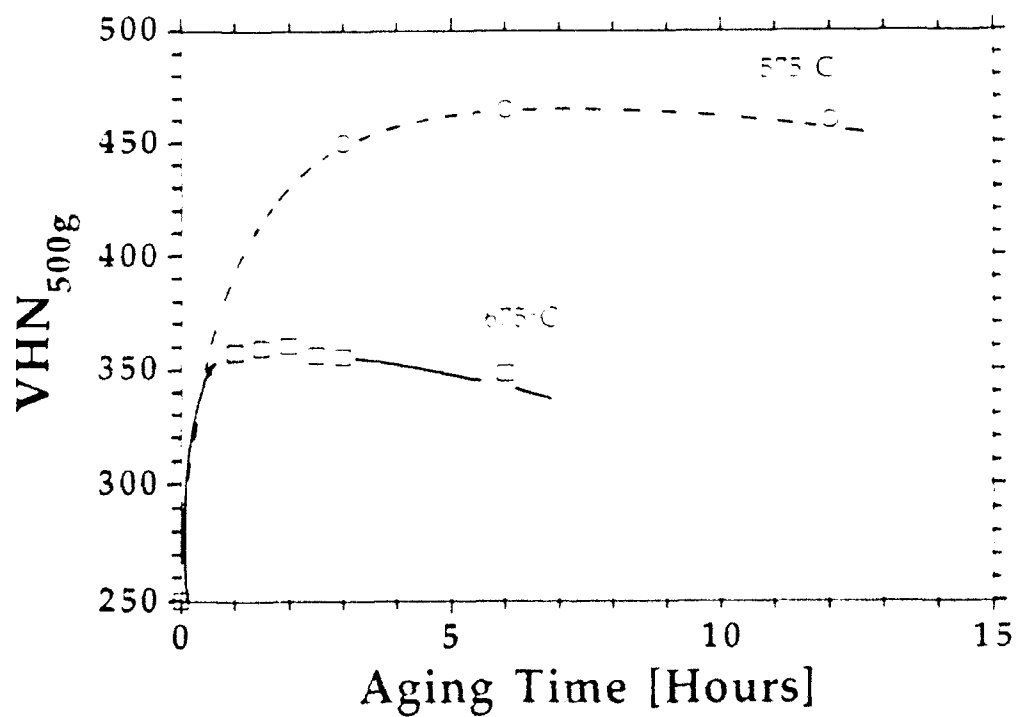


Figure 2. The age hardening response of the Ti-23-11 alloy in the solution-treated condition (1000°C/1hr, water quench).

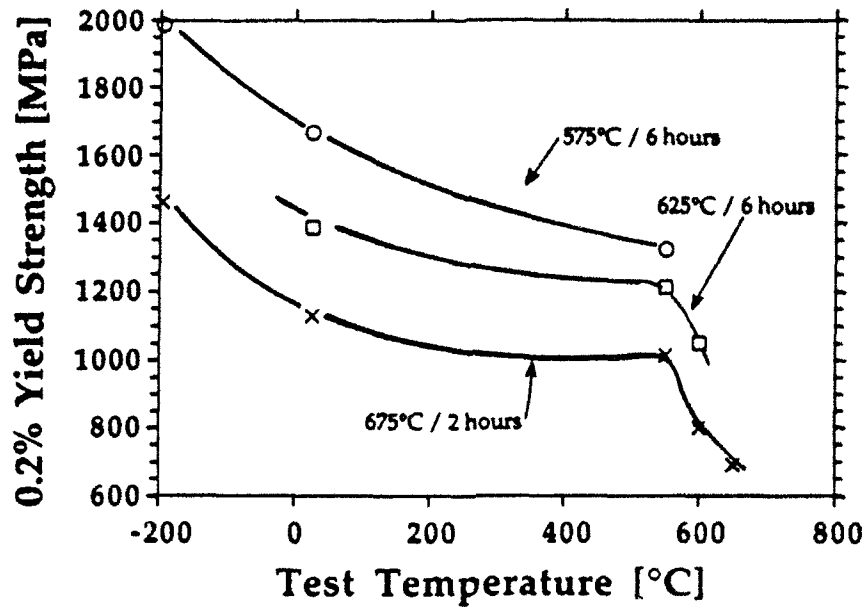


Figure 3. The temperature dependence of the yield strength for the Ti-23-11 alloy in a three heat-treated conditions.

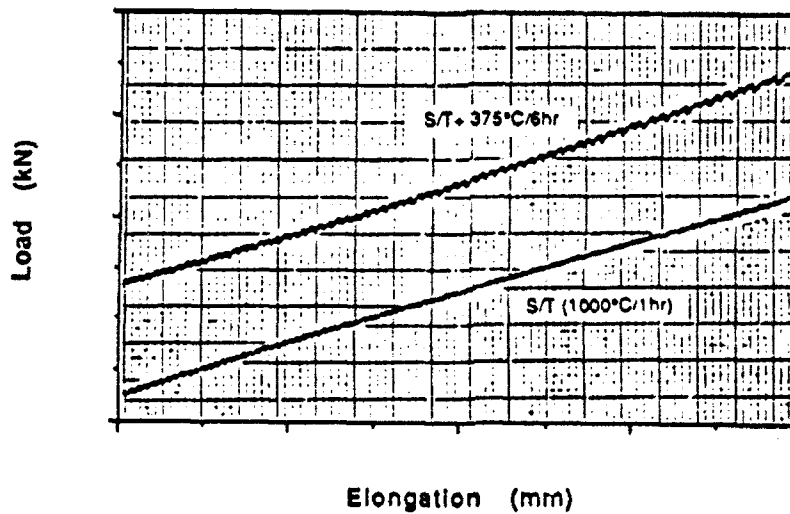


Figure 4. Jerky flow during testing at 327°C.

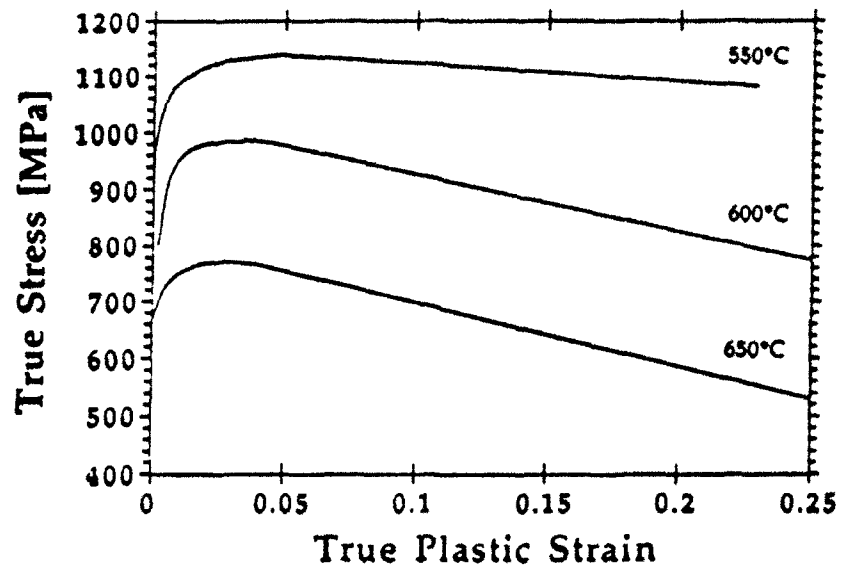


Figure 5. Stress-strain responses at 550°C exhibiting zero strain-hardening conditions, and at 600 and 650°C, respectively, exhibiting flow softening (negative strain-hardening). Specimen was solution-treated and aged at 675°C for 2 hrs.

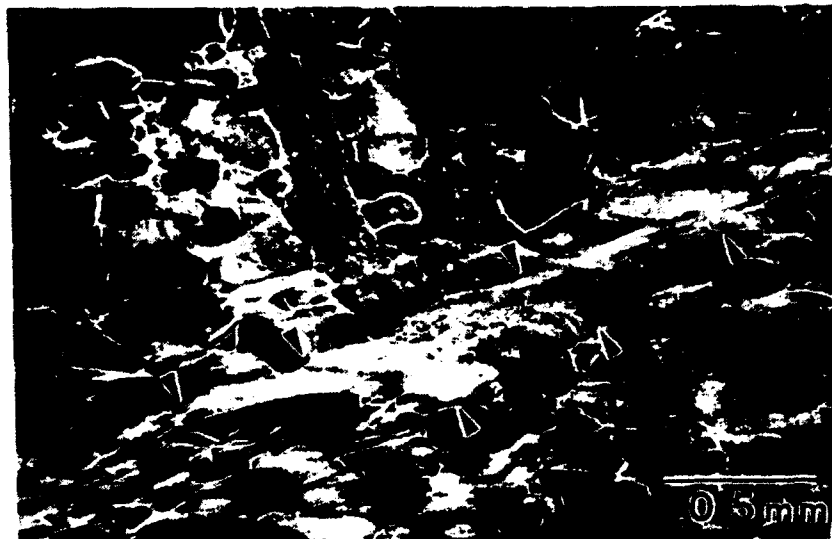


Figure 6. Optical micrograph of an as-deformed cross sectioned sample exhibiting localized flow instability within deformed pancake-shaped grains; see arrows.

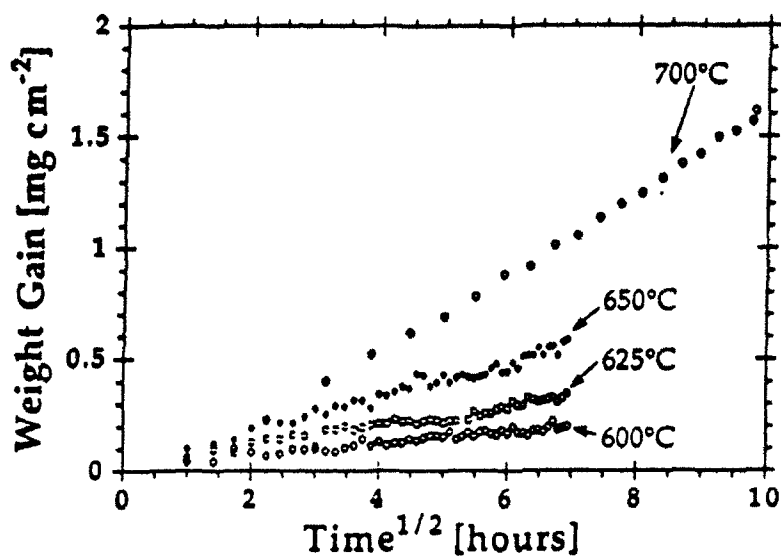


Figure 7. Weight-gain histories for Ti-23-11 oxidized in laboratory air between 600 and 700°C for up to 96 hours.

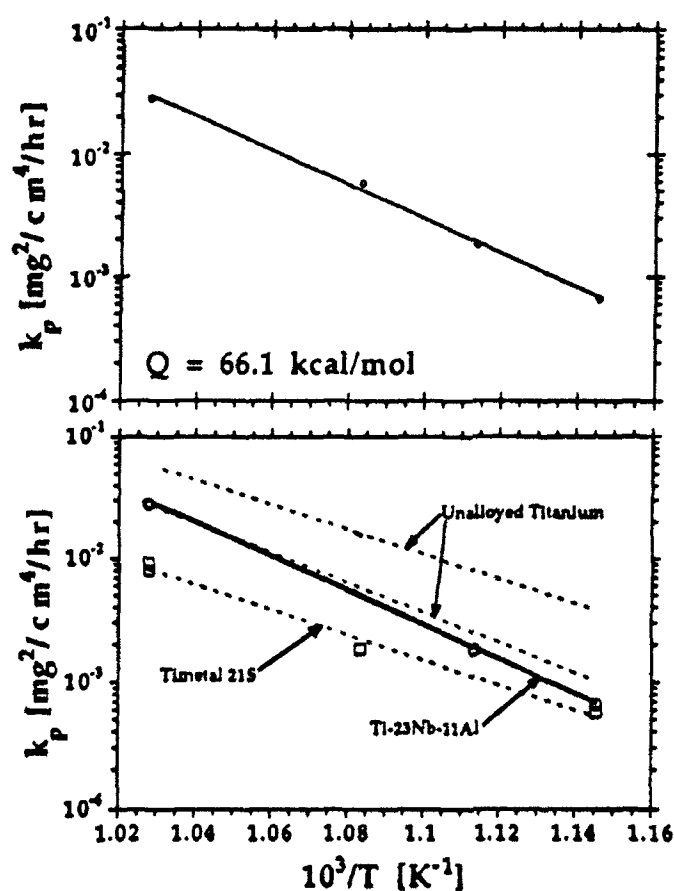


Figure 8. Arrhenius plot of parabolic rate constants for (a) Ti-23-11 oxidized in laboratory air between 600 and 700°C for up to 96 hours. Also included (b) are the parabolic rate constants for Ti-15Mo-2.7Nb-3Al-0.2Si (Timetal 21S) and unalloyed titanium after ref. 20.